THE JOURNAL OF PHYSICAL CHEMISTRY B

pubs.acs.org/JPCB Article

Viscoelasticity of Nanosheet-Filled Polymer Composites: Three Regimes in the Enhancement of Moduli

Wei Hong, Jiaping Lin,* Xiaohui Tian, and Liquan Wang*

Cite This: J. Phys. Chem. B 2020, 124, 6437−6447 Read Online

ACCESS | Metrics & More | Article Recommendations | Supporting Information

ABSTRACT: We employed nonequilibrium molecular dynamics simulations to elucidate the viscoelastic properties of nanosheet (NS)-filled polymer composites. The effects of NS loadings and NS−polymer interaction on viscoelasticity were examined. The simulation results show that the NS-filled polymer composites exhibit an enhanced storage modulus and loss modulus as the NSs are loaded. There are three regimes of the enhanced process based on the NS loadings. At lower NS loadings, the motion of polymers slows down owing to the interaction between NSs and polymers, and the polymer chains generally follow the Rouse dynamics. As the NS loadings increase, the polymer chains are confined between NSs, leading to a substantial increment in dynamic moduli. At higher NS loadings, a transient network is formed, which strengthens the dynamic moduli further. In addition, the attractive NS−polymer interaction can improve the dispersion of NSs and increase the storage and loss moduli. The present work could provide essential information for designing high-performance hybrid polymeric materials.

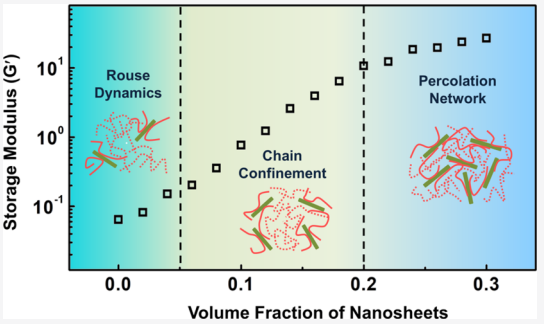

1. INTRODUCTION

The addition of organic/inorganic nanofillers including carbon black, silica, graphene, clay, and carbon nanotube into polymer matrixes can provide materials significantly enhanced properties such as viscoelasticity, electrical conductivity, flame retardation, and thermal conductivity.[1−6] The viscoelasticity, an essential class of properties, plays a dominative role in the processing and application of polymer nanocomposites (PNCs). When subjected to a low degree of strain, the nanocomposites usually show a distinct rheological response that deviates from the classical theory of linear viscoelasticity. The enhancement in the storage moduli (G') and loss moduli (G'') is usually more pronounced at low frequencies, and G' is more significantly enhanced than G''. However, there is much controversy over the issue of understanding the universal appearance and underlying mechanism.[7] For example, the solidlike behaviors observed in PNCs at low frequencies could be attributed to either the jamming of particles or the percolation network. Hence, an examination of the viscoelastic properties of these kinds of nanocomposites is crucial in both fundamental research and engineering applications.

The shape of nanofillers plays a role in the viscoelasticity of PNCs. Liu et al. examined the geometrical effect on the properties of polyethylene nanocomposites by constructing five different carbon forms, including graphene, buckyball, nanodiamond, X-shaped single-walled carbon nanotube (SWNT) junction, and Y-shaped SWNT junction.[8] They found that the surface-area-to-volume ratio of nanoparticles (NPs) plays the dominant role in both static and dynamical properties of polymer matrixes. Among all the abovementioned NPs, two-dimensional graphene sheets bear the largest ratio of surface area to volume and have the strongest interaction with the polyethylene matrix. PNCs containing two-dimensional nanosheets (NSs), as a vital branch of nanocomposites, have attracted considerable interest because of the characteristic topological structure of NSs.[9−14] To date, much effort was made to improve the viscoelastic properties of NS-based PNCs via increasing the dispersion of NSs in the polymer matrix.[15−23] Tang and coauthors investigated the effect of graphene dispersion on the mechanical properties of epoxy resins and found that good dispersion of graphenes can lead to increased strength and fracture toughness of the epoxy resins.[24] Zhang et al. studied the effect of surface chemistry of graphene on the rheological property of polymethylmethacrylate composites.[25] They found that graphene sheets with higher oxygen contents can be well dispersed in the polymer matrixes, and the corresponding composites exhibit a higher storage modulus and complex viscosity as well as a smaller rheological percolation threshold. Sadeghipour et al. investigated the effects of modified and nonmodified clay on the rheological properties of high-density polyethylene.[26] It was found that the nonmodified clays increase the elastic behavior, yet the

Received: May 13, 2020
Revised: June 24, 2020
Published: July 1, 2020

https://dx.doi.org/10.1021/acs.jpcb.0c04235
J. Phys. Chem. B 2020, 124, 6437−6447

modified clays increase the viscose behavior of the composites because of increased interactions with the matrix and partial intercalation. What is noteworthy is that the increase in the interaction between the NS and the polymer can not only achieve a good dispersion of NSs but also exert retardation on the dynamics of polymer chains.

Apart from the experiments, theoretical simulations, including molecular dynamics (MD),[27−29] Brownian dynamics,[30,31] and dissipative particle dynamics,[32−34] have been applied to investigate the dynamics and viscoelasticity of PNCs. For instance, Smith et al. utilized equilibrium MD simulations to investigate the viscoelasticity of model PNCs and found that the addition of NPs can strongly perturb the viscoelastic properties of the matrix polymers.[29] In contrast to equilibrium MD, nonequilibrium MD simulations can potentially reduce the computer load by producing a signal considerably larger than the background thermal noise. Li et al. performed nonequilibrium MD simulations to study the effect of interfacial chemical coupling on the viscoelasticity of nanocomposites under oscillatory shear and found that the formation of chemical coupling can weaken the "Payne effect".[35] Lin and coauthors employed the nonequilibrium MD to investigate the mechanical and viscoelastic properties of NP-tethering polymers and found that the tethering polymers exhibit an improved tensile modulus and improved dynamic moduli compared to the pure polymers as well as the blends of NPs and polymers.[36,37]

Several MD simulation studies on structural and dynamical properties of NS−polymer systems, which are strongly associated with viscoelasticity, have been reported recently.[38−41] Among them, Bačová and co-workers performed atomistic MD to investigate edge-functionalized graphene dispersed in low-molecular-weight polymer matrixes.[40] Strong structural and dynamical heterogeneities were observed, and the motions of the polymer were slowed down in the adsorbed layers close to the graphene. Until now, however, only limited simulation studies are available for the viscoelasticity of NS-based PNCs. The dynamics of polymers in NS-based PNCs, which may deviate from the classical Rouse model, is unclear. In addition, the physical origin of improved viscoelasticity in the NS-based PNC systems is not well understood. It is still necessary to utilize the coarse-grained MD simulation to bridge the gap between the viscoelastic and dynamic properties of NS−polymer systems. The success of nonequilibrium MD simulations makes them ready to be applied to investigate the viscoelastic properties of NS-based PNCs.

In the present work, we performed nonequilibrium MD simulations to investigate the oscillatory viscoelasticity of NS-based PNCs. The effects of NS contents and interactions between NSs and polymers on the viscoelasticity of NS-based PNCs were examined. It was found that the dynamic moduli can be enhanced by increasing the content of NSs and the NS−polymer attraction. We discovered that the enhancement of dynamic moduli could be divided into three regimes in terms of the NS loadings, which are associated with the Rouse dynamics, chain confinement, and percolation network. The present study can establish linkages between the dynamic behavior and viscoelastic properties of NS-based PNCs and could provide essential information for designing advanced hybrid nanomaterials.

2. METHODS AND THE MODEL

We employed nonequilibrium MD simulations to study the viscoelasticity of NS-based PNCs in melted states. A coarse-grained model of NS-based PNCs was first constructed, which is shown in Figure 1. Each polymer is modeled as a linear chain

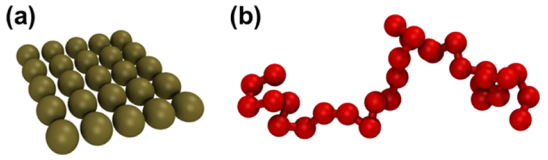

Figure 1. Coarse-grained models of (a) NS and (b) polymer. The polymer is a bead-spring chain with 30 beads, and the NS is a square sheet with 25 beads.

consisting of L beads, where each bead represents a cluster of monomers.[42−44] Each NS is modeled as a square sheet with N beads. All beads in the sheet move together as a rigid body.[45] The mass and diameter of each polymer/NS bead are set as m and σ, respectively. The potentials in the present MD simulations include the bonding potential U_{bond} and the nonbonding potential U_{ij}, which are given by the finitely extensible nonlinear elastic potential and modified Lennard-Jones (LJ) 12:6 potential,[46,47] respectively. In the LJ potential, the cutoff distance r_{ij}^{c} determines whether the interaction between beads i and j is attractive ($r_{ij}^{c} > 2^{1/6}\sigma$) or repulsive ($r_{ij}^{c} < 2^{1/6}\sigma$). In this work, the cutoff distance is fixed at 2.5σ (attractive) for the polymer−polymer interaction. The cutoff distance is set to be $2^{1/6}\sigma$ (repulsive) for the NS−NS interaction to prevent the NSs from aggregation. The interaction parameters ε_{pp} (between polymer beads) and ε_{nn} (between NS beads) are fixed as 1.0ε for convenience. ε_{np} and r_{np}^{c} are varied to simulate the systems with various NS−polymer interactions, that is, strongly attractive, weakly attractive, and repulsive interactions. All physical quantities in the simulations adopt reduced units. The units of energy, length, and mass are defined by ε, σ, and m, respectively. The time unit τ is obtained by $\tau = (m\sigma^2/\varepsilon)^{1/2}$. In principle, all reduced units can be converted into real units.[48] The details of the MD method can be found in Section S1 of the Supporting Information.

Following our previous work, the nonequilibrium MD simulation was adopted to simulate the NS-based PNCs subjected to an oscillatory strain.[36] The SLLOD equation of motion, which is the most widely used in the shearing systems, is implemented. We employed a "box deforming" technique to induce a shear field instead of Lees−Edwards "sliding brick" boundary conditions.[49,50] A deforming-box implementation of the SLLOD algorithm was adopted to produce a shear flow in the x-direction and a velocity gradient in the y-direction.

$$\frac{\mathrm{d}\mathbf{r}_i}{\mathrm{d}t} = \mathbf{v}_i + \mathbf{e}_x\dot{\gamma}\mathbf{r}_{i,y}$$

$$m_i\frac{\mathrm{d}\mathbf{v}_i}{\mathrm{d}t} = \mathbf{f}_i - m_i\mathbf{e}_x\dot{\gamma}\mathbf{v}_{i,y} \quad (1)$$

where $\mathbf{f}_i$, $\mathbf{r}_i$, and $\mathbf{v}_i$ are the force, position, and velocity of bead i, respectively. $\mathbf{e}_x$ is the normalized vector along the x-direction. $\mathbf{v}_{i,y}$ and $\mathbf{r}_{i,y}$ are the magnitudes of the corresponding vectors, where the subscript i denotes bead i and y represents the y-component of the vector. $\dot{\gamma}$, called the shear rate, is the time derivative of the shear strain γ. As an alternating strain was

https://dx.doi.org/10.1021/acs.jpcb.0c04235
J. Phys. Chem. B 2020, 124, 6437−6447

imposed on the simulation box, the stress was monitored simultaneously. When the equilibrium is achieved, both strain and stress alter sinusoidally, but the strain lags behind the stress. The expressions are as follows

$$\gamma = \gamma_0 \sin(\omega t) \tag{2}$$

$$\sigma_{xy} = \sigma_0 \sin(\omega t + \delta) \tag{3}$$

The stress consists of two components, that is, G' sin ωt and G'' cos ωt. Here, G' and G'' are the storage modulus and loss modulus, respectively. They are given by

$$G' = \frac{\sigma_0}{\gamma_0}\cos(\delta), \qquad G'' = \frac{\sigma_0}{\gamma_0}\sin(\delta) \tag{4}$$

We can obtain σ_{xy} readily through the tensor version of the virial theorem

$$\sigma = \frac{1}{V}\left\langle \sum_i m\mathbf{v}_i\mathbf{v}_i + \frac{1}{2}\sum_{i\neq j}\mathbf{r}_{ij}\mathbf{F}_{ij} \right\rangle \tag{5}$$

Here, V is the volume of the simulation box and the angular bracket denotes the ensemble average.

In the present work, the length L of the polymers in the matrix is 30, and each NS contains N = 25 beads to meet the experiments where the size of the NS is comparable to or larger than the chain dimensions.[6,13] The distance between adjacent beads of the NS is fixed as 0.75σ so that the square NS has a width of 3σ, which is in the order of the length scale of the polymers. For generating an initial configuration, an NS-based PNC system with a lower density ρ was first constructed within a large simulation box of $100 \times 100 \times 100\sigma^3$ and was then compressed until ρ = 0.45. Here, the density ρ is the ratio of the volume of beads (including NS and polymer beads) to the volume of the simulation box. The isothermal−isobaric (NPT) ensemble was applied to equilibrate the compressed box by using the Nose−Hoover thermostat and barostat. Therefore, the size of the box for different systems was varied to maintain the fixed density ρ. For instance, the edge lengths of the box are 24.77σ for the pure polymer system. It was proved that the box size effects were eliminated. The velocity Verlet algorithm was adopted to integrate the equations of motion. We carried out 8×10^7 MD steps with a time step of $\Delta t = 0.004\tau$ for all the structures. After the equilibrium structures were obtained, the nonequilibrium MD simulations were performed by changing the cubic box to a triclinic one.

3. RESULTS AND DISCUSSION

The present work focuses on the linear viscoelasticity of NS-based PNCs, which is organized as follows. We first investigated the effect of volume fraction of NSs on the viscoelastic properties of NS-based PNCs. Then, we examined the effects of NS−polymer interactions on the viscoelastic properties. The PNCs filled with spherical NPs have received extensive research over the past decades.[7] The shape of the nanofiller has a substantial impact on the viscoelasticity of PNCs. Therefore, we made a comparison of the viscoelasticity between NS-based and NP-based PNCs to reveal the uniqueness of the NS. Finally, a comparison with the existing experimental observations was made.

3.1. Enhanced Dynamic Moduli with the NS Loaded.

It has been documented that the dispersion of NSs has a marked influence on the linear viscoelasticity of NS-based PNCs. In this subsection, we focused on the linear viscoelasticity of NS-based PNCs with attractive NS−polymer interactions that can enhance the dispersion. Therefore, the interaction strength ε_{np} between NSs and polymers and the cutoff distance r_{np}^c were set as 5.0ε and 2.5σ, respectively. The equilibrium structures of NS-based PNCs with various volume fractions of NSs are shown in Figure S1 of the Supporting Information. As shown, the NSs have a good dispersion in the polymer matrixes.

The linear viscoelastic region of the PNC systems is determined via dynamic amplitude scan measurements so as not to destroy the structures of the samples. Figure 2 shows the dependence of the storage modulus G' and loss modulus G'' of PNCs on the strain under shear frequencies of $\omega = 0.01\tau^{-1}$ for samples with various volume fractions of NSs. For ϕ = 0, that is, pure polymers, G' almost shows no strain dependence over the range of strains studied, indicating a very weak Payne effect.[35,49] However, G' of NS-based PNCs becomes sensitive to the oscillation amplitude. The strain independence at small amplitudes and strain dependence at large amplitudes were observed. The equilibrium structures are not destroyed under small strain, resulting in the plateau of G' and G''. The decrease in G' and G'' occurs under large strain, which derives from the increase of energy dissipation and structural breaking. It is noteworthy that there is a peak for G'' of systems with an NS loading larger than 0.2, which indicates the formation of the interpenetrating network. In addition, both G' and G'' increase, and the linear viscoelastic regions become narrow with the increase of NS loadings. The result manifests that the NS-based PNCs exhibit the Payne effect, which is enhanced with the increase of NS loadings. To guarantee the linear viscoelastic behaviors in the following simulations, a strain amplitude of γ = 0.05 proved in the linear regime (see Figure 2) is applied.

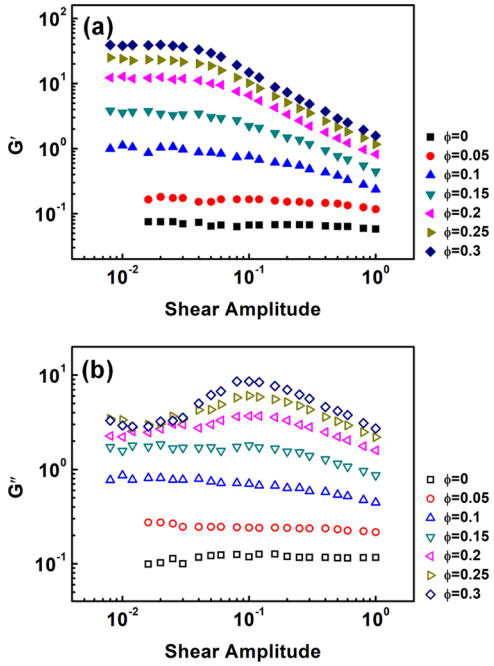

Figure 2. Dynamic (a) storage moduli G' and (b) loss moduli G'' as a function of strain amplitude for the NS-based PNCs with various volume fractions of NSs under a shear frequency of $\omega = 0.01\tau^{-1}$.

https://dx.doi.org/10.1021/acs.jpcb.0c04235
J. Phys. Chem. B 2020, 124, 6437−6447

Figure 3a,b shows the plots of storage modulus G' and loss modulus G'' versus shear frequency ω for NS-based PNCs.

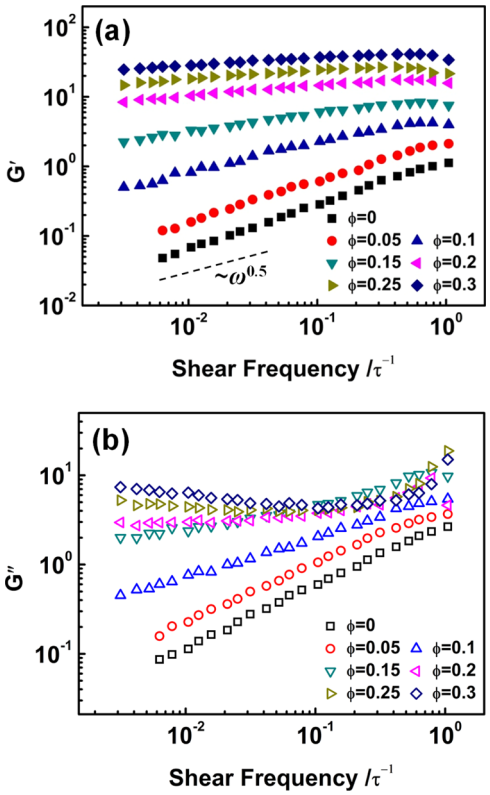

Figure 3. Dynamic (a) storage moduli G' and (b) loss moduli G'' as a function of shear frequency for the NS-based PNCs with various volume fractions of NSs.

The results at lower frequencies are not presented because of the sharp thermal fluctuation. As shown in the figure, both G' and G'' of NS-based PNCs increase with the increase of the NS loading and are larger than those of pure polymers ($\phi = 0$). For the pure polymer system, the relationship, $G' \sim G'' \sim \omega^{0.5}$, was observed at intermediate frequencies ($\tau_R^{-1} < \omega < \tau_0^{-1}$, where τ_R and τ_0 denote the Rouse relaxation time and monomer relaxation times, respectively), indicating that the polymer chains generally follow the Rouse dynamics.[51] The frequencies applied are not low enough such that the terminal behaviors were not observed in the pure polymers. The G' and G'' profiles of PNCs with an NS loading of $\phi = 0.05$ show similarity in shape to those of the pure polymers. Both storage and loss moduli of pure polymers can be shifted by an almost constant factor across the entire frequency range to approach those of PNCs with $\phi = 0.05$. At intermediate NS loadings ($\phi = 0.1$ and 0.15), the G's of these PNCs display a power-law dependence on frequencies in which the exponent is less than 0.5, deviating from the Rouse dynamics. The power-law exponent decreases with the increase of NS loadings, which is ascribed to the lack of complete relaxation of polymer chains in the presence of NSs. In addition, the NSs are constrained and incapable of freely rotating when subjected to a small amplitude shear. At higher NS loadings ($\phi \geq 0.2$), the PNCs show solidlike behaviors ($G' \sim \omega^0$), indicating the formation of a transient percolation network in which the movement of polymers and NSs is highly restrained.

3.2. Origin of Enhanced Dynamic Moduli. In order to get a deep insight into the physical origin of enhanced viscoelasticity of NS-based PNCs, we evaluated the relaxation time for polymer chains in the pure polymers and PNCs. To this end, we obtained the normal modes for each polymer chain given by[33,51]

$$\mathbf{X}_p(t) = \sqrt{\frac{2}{L}} \sum_{i=1}^{L} \cos\left(p\pi \frac{i - 1/2}{L}\right) \mathbf{R}_i(t) \quad (6)$$

where p is the mode and $\mathbf{X}_p(t)$ is the pth normal mode of the polymer chain. $\mathbf{R}_i(t)$ denotes the position vector of the ith bead at time t. The time correlation function of the normal modes is given as $\mathbf{A}_p(t)$

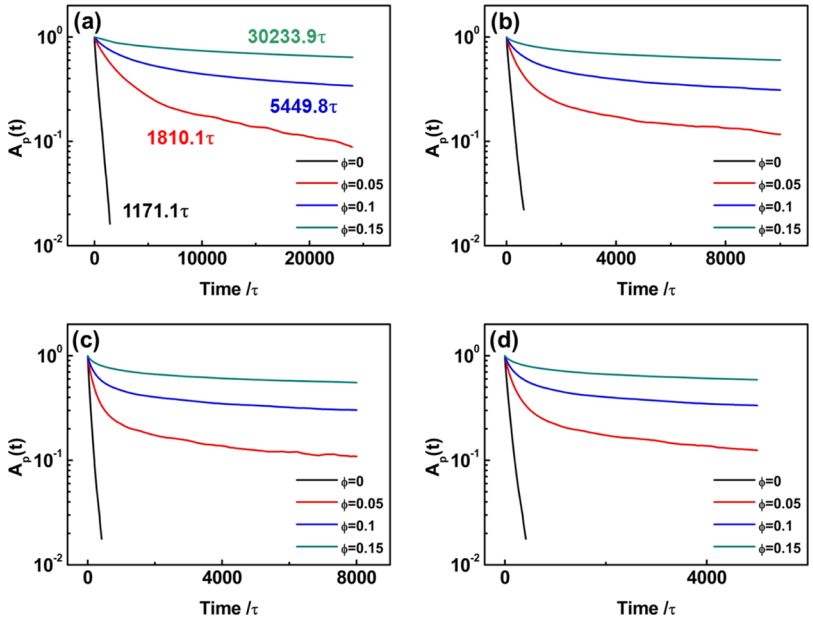

Figure 4. Relaxation spectra $\mathbf{A}_p(t)$ of the polymer chains in NS-based PNCs with various volume fractions of NSs for the four slowest Rouse modes: (a) $p = 1$, (b) $p = 2$, (c) $p = 3$, and (d) $p = 4$. The relaxation times for $p = 1$ are highlighted in the plots.

https://dx.doi.org/10.1021/acs.jpcb.0c04235
J. Phys. Chem. B 2020, 124, 6437−6447

$$\mathbf{A}_p(t) = \frac{\langle \mathbf{X}_p(t)\cdot\mathbf{X}_p(0)\rangle}{\langle \mathbf{X}_p(0)\cdot\mathbf{X}_p(0)\rangle} \tag{7}$$

Here, the angular bracket denotes the ensemble average over all polymer chains and time. We can obtain the relaxation time by fitting $\mathbf{A}_p(t)$ to a decaying exponential function. For the pure polymer, the spectra for various modes can be well represented by a stretched exponential function

$$\mathbf{A}_p(t) = \exp[-(t/\tau_p)^{\beta}] \tag{8}$$

where the exponent β is the stretching exponent, characterizing the "heterogeneous" nature of the dynamics. τ_p is the relaxation time for the pth mode.

For the NS-based PNCs, we found that the function $\mathbf{A}_p(t)$s show a long-time tail, which cannot be well fitted by the stretched exponential function. Ultimately, a modified equation proposed earlier was adopted to fit the spectra across various modes,[27,29] which is

$$\mathbf{A}_p(t) = C\exp[-(t/\tau_p)^{\beta}] + (1 - C)\exp[-t/\tau_1] \tag{9}$$

where C and τ_1 are the additional fitting parameters representing a decay of two exponential-like functions.

We have computed the function $\mathbf{A}_p(t)$s of the polymer chains in systems with ϕ = 0, 0.05, 0.1, and 0.15 for the four slowest modes (p = 1, 2, 3, and 4). The relaxation times of the whole chain τ_1 (p = 1) are obtained by fitting the curves with eq 8 for pure polymers and with eq 9 for PNCs. The results are shown in Figure 4. Note that the relaxation of PNCs with higher NS loadings is so prolonged that we cannot monitor the relaxation process completely (the relaxation data for PNCs at a long time scale are not shown for visual clarity). For p = 1,$\mathbf{A}_p(t)$ in the pure polymer shows a single exponential decay, while those in NS-based PNCs exhibit a double exponential decay (see Figure 4a). The decay of the time autocorrelation function slows down gradually with the increase of NS loadings. The longest relaxation times are 1171.1τ, 1810.1τ, 5449.8τ, and 30,233.9τ for the PNCs with NS loads of ϕ = 0, 0.05, 0.1, and 0.15, respectively (see Figure 4a). For p = 2, 3, and 4, the relaxation spectra of polymer chains in the pure polymer and NS-based PNCs exhibit a similar tendency (see Figure 4b–d). It is evident that the addition of NSs increases the relaxation times, and the relaxation times have a dramatic increase at middle NS loadings (ϕ = 0.1 and 0.15). As shown in Figure 4, there is a long-time tail in the decay of the time autocorrelation for the PNCs. The second relaxation time could be related to the dynamic adsorption–desorption process of polymer chains from NS surfaces.

Rouse theory elaborates that the storage and loss moduli are of quadratic and linear growth with respect to the relaxation time, respectively.[51] We compared the G' and G'' values of pure polymers with those of PNCs with ϕ = 0.05, which is presented in Figure S2. As shown, the relaxation time increases by 1.55 times, and therefore, the G' and G'' values of PNCs with ϕ = 0.05 are about 1.55^2 and 1.55 times higher than those of the pure polymer system, respectively. The data are consistent with the results predicted by the Rouse theory. Such an analysis manifests that the polymer chains generally follow the Rouse dynamics at a lower NS loading (ϕ = 0.05). The substantial increase of relaxation time at middle NS loadings (ϕ = 0.1 and 0.15) could be attributed to the chain confinement between NSs.

At higher NS loadings (ϕ = 0.2, 0.25, and 0.3), the storage modulus becomes frequency-independent (see Figure 3), and the relaxation dynamics is extremely slow, indicating a solidlike rheological behavior and the formation of NS networks. Therefore, there should be a critical NS concentration above which the microstructure has a sudden change. To further investigate the influence of NS loading on the viscoelasticity, we examined the dependence of the enhancement in low-frequency G' on the NS loadings. Figure 5a shows the low-

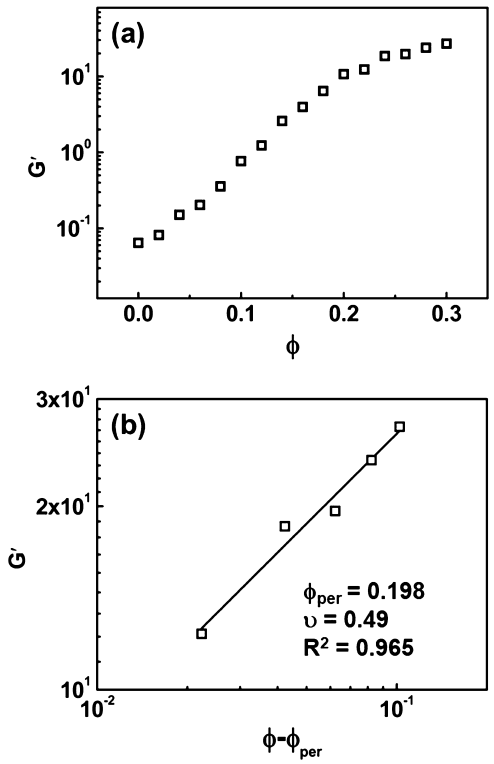

Figure 5. (a) Storage modulus G' of the NS-based PNCs as a function of NS loading at $\omega = 0.01\tau^{-1}$ and (b) log–log plot of G' vs reduced volume fraction of NSs. The solid line is the fitting curve, and the fitting parameters are highlighted in the plot.

frequency G' under a shear frequency of $0.01\tau^{-1}$ as a function of the NS loadings. As shown in the figure, G' increases monotonically with the increase of the NS loading. However, the extent of increase is related to the NS loadings. G' increases slightly at lower NS loadings, followed by a dramatic increase at middle NS loadings. The viscoelasticity of PNCs at lower loadings is dominated by the Rouse relaxation of polymers, while chain confinement leads to slow relaxations and substantial enhancements in elasticity at middle loadings. However, there is only a slight and steady increase in storage modulus at higher loadings. The solidlike viscoelastic response at higher loadings arises from the formation of a percolation network in PNCs (see Figure 3). Based on the above analysis, we can use a power-law relation to evaluate the rheological percolation threshold according to the percolation theory[13]

$$G' \propto (\phi - \phi_{per})^{\upsilon} \tag{10}$$

where G' is the storage modulus at a low frequency, υ is the critical exponent, and ϕ and ϕ_{per} are the NS volume fraction and percolation threshold, respectively. The percolation threshold can be evaluated by applying eq 10, which is

https://dx.doi.org/10.1021/acs.jpcb.0c04235
J. Phys. Chem. B 2020, 124, 6437–6447

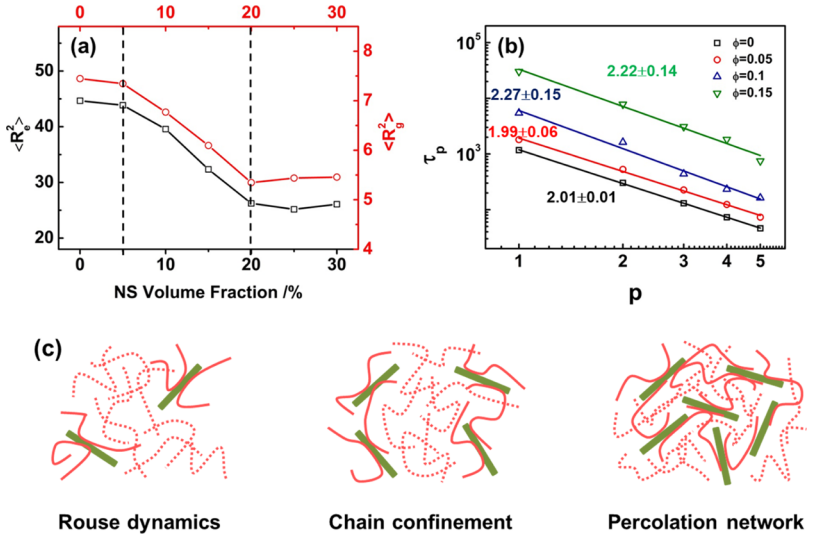

Figure 6. (a) Mean square end-to-end distance $\langle R_e^2 \rangle$ and the mean square radius of gyration $\langle R_g^2 \rangle$ as a function of the NS loadings. (b) Relaxation time τ_p as a function of modes p for the five slowest Rouse modes in NS-based PNCs with various NS volume fractions. (c) Schematic illustration of the NS-based PNCs evolving from low-to-intermediate-to-high loadings. The red solid line and red dashed line represent the adsorbed and free polymer chains, respectively. The NSs are represented as green rectangles.

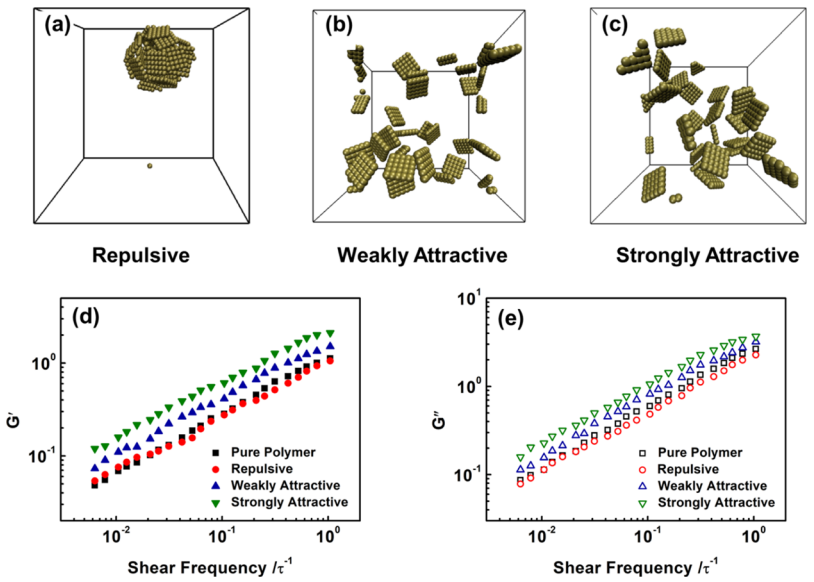

Figure 7. Equilibrium structures of NS-based PNCs at $\phi = 0.05$ with (a) repulsive, (b) weakly attractive, and (c) strongly attractive NS−polymer interactions. Frequency sweeps of (d) G' and (e) G'' in the pure polymers and NS-based PNCs at $\phi = 0.05$ with repulsive, weakly attractive, and strongly attractive NS−polymer interactions.

shown in Figure 5b. The calculated threshold fraction is about 0.198, above which the elastic plateau can be observed (see Figure 3). These results manifest the fact that NS-based PNCs with higher NS loadings form a percolating network structure and show solidlike viscoelastic behaviors.

To understand the mechanisms of enhanced viscoelasticity behavior, we examined the structural characteristic of the matrix polymer chains by calculating the mean square end-to-end distance $\langle R_e^2 \rangle$ and the radius of gyration $\langle R_g^2 \rangle$. The results are given in Figure 6a. As shown, the variation of $\langle R_e^2 \rangle$ and $\langle R_g^2 \rangle$ as a function of NS loading can be divided into three regions, that is, region I ($\phi \leq 0.05$), region II ($0.05 < \phi < 0.2$), and region III ($\phi \geq 0.2$). In region I, $\langle R_e^2 \rangle$ and $\langle R_g^2 \rangle$ decrease slightly with the increase of NS loadings, indicating that the structures remain stable, and the addition of NSs has a less marked effect on the chain stretching. One can see that both $\langle R_e^2 \rangle$ and $\langle R_g^2 \rangle$ decrease sharply with the increase of NS loading in region II, demonstrating the confinement of polymer chains. $\langle R_e^2 \rangle$ and $\langle R_g^2 \rangle$ remain almost unchanged in region III, suggesting that the structures remain stable and the percolation network forms. In addition, the relaxation time as a function of the mode p is shown in Figure 6b. For the pure polymers and the PNCs with a lower NS loading ($\phi = 0.05$), the relaxation time τ_p scales with the mode as $\tau_p \sim p^{-2}$, which is consistent with the prediction of the Rouse model. This indicates that the influence of NSs on the dynamics of matrix polymers is the same for all length scales. However, for the PNCs with intermediate NS loadings ($\phi = 0.1$ and 0.15), the scaling relations $\tau_p \sim p^{-2.27}$ and $\tau_p \sim p^{-2.22}$ are observed,

https://dx.doi.org/10.1021/acs.jpcb.0c04235
J. Phys. Chem. B 2020, 124, 6437−6447

indicating the slight deviation from the Rouse model prediction.

From the above results, our implementations divide the enhancement of dynamic moduli into three regimes, that is, the Rouse dynamics at lower NS loadings, chain confinement at intermediate NS loadings, and percolation network at higher NS loadings. Figure 6c shows the schematic illustration of the typical topological structure of PNCs at various NS loadings. At lower NS loadings, the polymer chains adsorb on the surfaces of NSs because of the attractive interaction between the NS and polymer. The adsorption and desorption behaviors reach the dynamic balance, and the motion of polymer chains slows down uniformly, resulting in the "dynamic homogeneity". At intermediate NS loadings, the $\langle R_e^2 \rangle$ and $\langle R_g^2 \rangle$ values of matrix chains start to decrease sharply, demonstrating that the polymer chains are confined between the NSs. At higher NS loadings, there are sufficient NSs to connect the single chains, resulting in the formation of a percolation network.

3.3. Effect of NS−Polymer Interactions. In this subsection, we focused on the effect of NS−polymer interactions on the viscoelasticity of NS-based PNCs. Three kinds of NS−polymer interactions, including strongly attractive, weakly attractive, and repulsive interactions, were considered. The type of NS−polymer interactions is determined by the cutoff distance r_{np}^c and the interaction parameter ε_{np} in the LJ potentials. r_{np}^c was set as 2.5σ for the attractive systems (including strong and weak attractions) and $2^{1/6}\sigma$ for the repulsive system. In addition, the values of ε_{np} were set as 5.0ε and 3.0ε for the strongly attractive and weakly attractive systems, respectively. A PNC system with an NS volume fraction of $\phi = 0.05$, obeying the Rouse dynamics, was chosen in the following studies.

Figure 7a−c shows the equilibrium structures for the NS-based PNCs with strongly attractive, weakly attractive, and repulsive NS−polymer interactions. As shown in the figure, the NSs are uniformly dispersed in the weakly attractive and strongly attractive systems (see Figure 7b,c), while the NSs tend to agglomerate in the repulsive system (Figure 7a). These observations manifest that the attractive interaction between the NS and polymer can improve the dispersion of NSs. Figure 7d,e shows G' and G'' as a function of shear frequency for these three systems, respectively. As shown, both G' and G'' for these three systems exhibit similar tendencies as the response of pure polymers to shear frequency. The G' and G'' of the strongly attractive system are larger than those of the weakly attractive and repulsive systems, and the moduli of the repulsive system are the smallest among the three systems and are comparable to those of pure polymers. The results demonstrate that the attractive NS−polymer interaction can enhance the G' and G'' of PNCs at lower NS loadings. For repulsive systems, the dynamics and viscoelasticity are not influenced dramatically because of the poor dispersion of NSs. In addition, we also observed that at a higher NS loading ($\phi >$ 0.05), the PNCs with the strongly attractive NS−polymer interaction exhibit enhanced G' and G'' compared to the PNCs with the weakly attractive and repulsive NS−polymer interactions.

The above enhancement in G' and G'' arises from the slowdown in the dynamics of the matrix polymers. To verify this, we calculated the time autocorrelations $\mathbf{A}_p(t)$ with $p = 1$ for PNCs with various NS−polymer interactions—the result is shown in Figure 8. $\mathbf{A}_p(t)$ of PNCs with the repulsive interaction remains a single exponential form, while those of

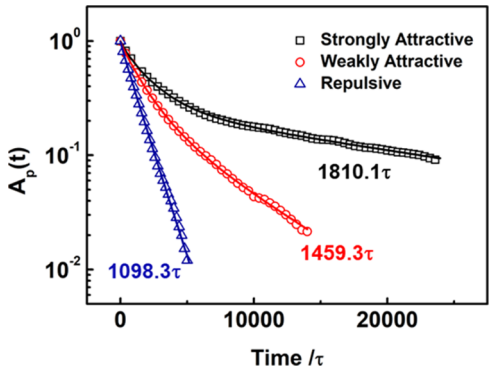

Figure 8. Relaxation spectra $\mathbf{A}_p(t)$ of the whole polymer chain in NS-based PNCs with strongly attractive, weakly attractive, and repulsive NS−polymer interactions. The solid lines are the theoretical fitting curves. The longest relaxation times are highlighted in the plot.

PNCs with the strongly attractive and weakly attractive interactions consist of two exponential functions. The relaxation time can be obtained by fitting the curves to eq 8 for the repulsive interactions or eq 9 for the two attractive interactions. The relaxation times are 1810.1τ, 1459.3τ, and 1098.3τ for the strongly attractive, weakly attractive, and repulsive systems, respectively. The Rouse time in the repulsive system is close to that in pure polymer systems (1171.1τ, see Figure 4a), which is attributed to the absence of the effective interaction between NSs and polymers. The relaxation time increases as the interaction changes from weak to strong attraction. These results verify that the NS−polymer attraction can suppress the motion of matrix polymers, which leads to an increase in relaxation time. It is noteworthy that the second relaxation time τ_1 in the weakly attractive system is much less than that in the strongly attractive system. These further demonstrate that the NS−polymer attraction can enhance the adsorption of polymers on NSs and, therefore, the moduli.

3.4. Comparison with NP-Based Nanocomposites. We have shown above that the storage and loss moduli are enhanced in the NS-based PNCs as compared with the pure polymers. Herein, we made a comparison of the viscoelastic properties between NS-based PNCs and widely studied NP-based PNCs. The PNCs filled with NPs, bearing a wide range of practical applications, have received considerable interest in the past decades.[3,7,33] In our simulation, the spherical NP was designed as a rigid dodecahedron composed of a center bead and 20 vertex beads (see Figure S3). The distance between adjacent vertex beads (i.e., the edge length of the dodecahedron) is fixed as 0.75σ, and therefore, the radius of the NP is ca. 1.05σ. The mass and diameter of each vertex bead are set as m and σ, respectively. The mass and diameter of the center bead are fixed as $5m$ and ca. 1.71σ, respectively. As such, the mass of the spherical NP is $25m$, which is equal to that of the NS. Additionally, to make the two systems comparable, the length of polymer chains in these systems was taken to be identical, and the volume fractions of the NSs and NPs were fixed to be 0.1. Because the attractive systems exhibit distinct viscoelasticity, the viscoelasticity of NS-based PNCs and NP-based PNCs with attractive interactions was explored by setting the interaction strength ε_{np} and cutoff distance r_{np}^c to be 5ε and 2.5σ, respectively.

Figure 9a shows G' and G'' of the NS-based and NP-based PNCs. The NSs and NPs disperse uniformly in the matrix polymers because of the attractive interaction (see the insets of

https://dx.doi.org/10.1021/acs.jpcb.0c04235
J. Phys. Chem. B 2020, 124, 6437−6447

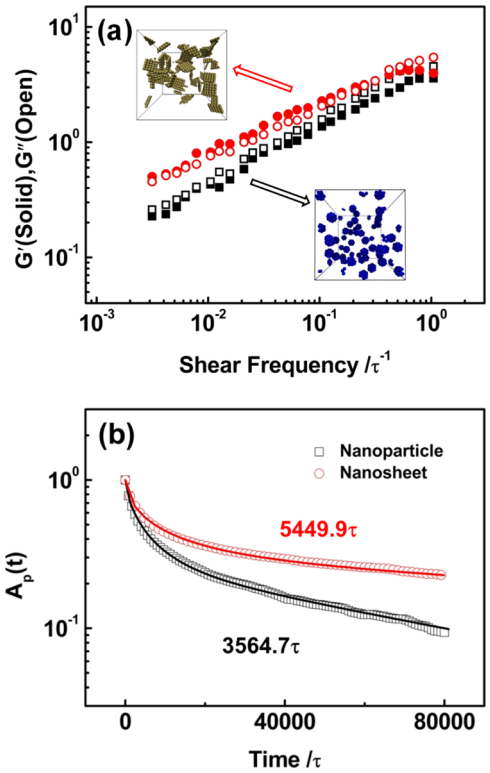

Figure 9. (a) Frequency sweep of G' and G'' in the NS-based and NP-based PNCs with $\phi = 0.1$. The insets show the equilibrium structures of NS-based and NP-based PNCs (the polymer beads are not shown). (b) Relaxation spectra $\mathbf{A}_p(t)$ of the whole polymer chain in the NS-based and NP-based PNCs. The solid lines are the theoretical fitting curves. The longest relaxation times are highlighted in the plot.

the figure). As can be seen, G'' is larger than G' for NP-based composites over the entire frequency regime, indicating liquidlike viscoelasticity. However, a crossover was observed in the NS-based composites, demonstrating that a solid-to-liquid transition occurs with the increase of frequency. In the NS-based systems, both G' and G'' are larger, and the power-law exponents for G' and G'' are smaller, as compared with NP-based systems. These results suggest that the NS-based PNCs exhibit enhanced viscoelastic properties relative to NP-based PNCs as the fillers and polymers are attracted.

Figure 9b shows the relaxation spectra of the slowest mode in NS-based and NP-based composites. It was found that the autocorrelation function in NP-based composites shows a double exponential decay, which is similar to the decay in NS-based composites. The relaxation time, obtained by fitting the curve to eq 9, is 3564.7τ. Compared with the relaxation time of the NP-based composites, the relaxation time of the NS-based system is much larger. Clearly, for equal particle loadings, the motion of polymer beads in NS-based PNCs is slower than that in NP-based PNCs, and therefore, the former exhibits higher storage and loss moduli than the latter. The slowdown in polymer dynamics is related to the larger surface-area-to-volume ratio of NSs and chain confinement between two-dimensional plates.

Moreover, the confinement of polymers in the NP-based system can be neglected when compared with that in NS-based composites, especially at higher loadings. In our simulations, the motion of polymers is highly restricted, and the NSs can form a perfect transient network at higher loadings. However, there is a striking difference between NS-based and NP-based PNCs. Pryamitsyn and Ganesan have used a nonequilibrium method to investigate the viscoelasticity of polymer−NP composites.[33] The relaxation dynamics of the normal modes show a single exponential decay and remain homogeneous at lower and higher NP loads. They found that the viscoelastic response at low frequencies is dominated by the particle jamming effects rather than the transient network. In short, NS-based PNCs have higher storage and loss moduli than NP-based PNCs at lower loadings because of the larger surface-area-to-volume ratio of the NS. At middle and higher loadings, the chain confinement and percolation network exist in NS-based PNCs, leading to the substantial enhancement in dynamic moduli. Different from NS-based PNCs, particle jamming effects dominate the viscoelastic response and lead to slow relaxations and enhanced moduli in NP-based PNCs.

3.5. Comparison with Existing Experimental Observations. Our study has shown that the NS-based PNCs exhibit the Payne effect, which is enhanced as the NS loadings increase. Similar results can be found in experiments on the clay- and graphene-based polymer composites. For example, Wu et al. studied the rheological behavior of poly(butylene terephthalate)/montmorillonite nanocomposites (PBT/MMT).[21] They found that with the addition of MMT, the linear viscoelastic region of PBT/MMT hybrids lessens gradually. For the PBT/MMT hybrid with higher MMT loadings, its linear viscoelastic region is much narrower than that of the PBT matrix. Gao et al. investigated graphene networks with a low percolation threshold in acrylonitrile−butadiene−styrene nanocomposites.[52] A pronounced reduction of G' with increasing strain was observed in their study. Moreover, they found that the linear viscoelastic regime decreases with increasing graphene content. These experimental observations are consistent with our simulation results, that is, the linear viscoelastic region in NS-based PNCs becomes narrower with the increase of NS loadings (see Figure 2).

In addition, we found that the NS-based PNCs show enhanced storage and loss moduli compared to the pure polymers, and the moduli can increase further with the increase of NS loadings. Some experimental observations in the literature are available to support these results.[1,12−15,25,52,53] For instance, Kim and Macosko studied the morphology and properties of polyester/exfoliated graphite nanocomposites.[13] They found that the shear modulus of the nanocomposites increases as the concentration of the graphite increases. Our simulation results also reveal that the NS-based PNCs form a percolation network at higher NS loadings. Similar results can be found in experiments.[13,14,25,53] For example, He and co-workers investigated the rheological behavior of epoxidized natural rubber−graphene composites.[14] They found that the storage modulus becomes frequency-independent at low frequencies, indicating the formation of a graphene network. The rheological threshold was determined to be 0.17% (volume fraction) according to the threshold theory.

In addition to the reproduction of general features of experimental findings for NS-based PNCs, the simulations reveal the microscopic origin of the viscoelasticity of polymeric systems to deepen the understanding of experimental observations. So far, the linear rheology of PNCs has many problems unsolved. For example, introducing NPs can retard the motion of matrix polymers. Experimentally, the origin of

https://dx.doi.org/10.1021/acs.jpcb.0c04235
J. Phys. Chem. B 2020, 124, 6437−6447

slow relaxation may be the physical or chemical absorption, particle jamming, polymer confinement, and so on. In the simulations, it is convenient to visualize the dispersion state and orientation behaviors of NSs in simulations (Figure 7a−c). Moreover, the dynamics and structural information of polymer chains can be elucidated easily (Figures 4 and 6a,b). Utilizing the nonequilibrium MD simulation, we discovered that the mechanisms underlying the viscoelasticity behavior could be divided into three aspects in terms of the NS loading, that is, the Rouse dynamics at lower NS loadings, chain confinement at intermediate NS loadings, and percolation network at higher NS loadings. Notably, the substantial enhancements in storage modulus can be observed at intermediate NS loadings because the polymer chains are confined between the NS platelets. Our simulations can give a more in-depth insight into the mechanisms of distinct viscoelasticity of PNCs with various NS loadings.

4. CONCLUSIONS

In the present work, the nonequilibrium MD simulations were conducted to study the viscoelastic properties of NS-based PNCs. The results show that the NS-based PNCs exhibit significantly enhanced storage and loss moduli compared to pure polymers. The effects of NS loading and NS−polymer interactions on the viscoelastic behavior of NS-based PNCs were examined. The storage and loss moduli were found to increase as the NS loadings increase. The enhancement of dynamic moduli can be divided into three regimes, which are related to the Rouse dynamics, chain confinement, and percolation network. The chain confinement at intermediate NS loadings results in the slow relaxations and substantial enhancements of storage moduli. The attractive interaction between NSs and polymers, favoring the excellent dispersion of NSs into the polymer matrix, further slows down the motion of polymer chains and enhances the viscoelasticity of PNCs. The simulations revealed the microscopic origin of distinct viscoelasticity of NS-based PNCs, and the gained results could provide information for designing advanced composites filled with two-dimensional organic/inorganic plates.

■ ASSOCIATED CONTENT

Supporting Information

The Supporting Information is available free of charge at https://pubs.acs.org/doi/10.1021/acs.jpcb.0c04235.

Coarse-grained MD, equilibrium structures of NS-based polymer composites, and validation of the Rouse dynamics of polymers in NS-based polymer composites with a low volume fraction of NSs (PDF)

■ AUTHOR INFORMATION

Corresponding Authors

Jiaping Lin − *Shanghai Key Laboratory of Advanced Polymeric Materials, Key Laboratory for Ultrafine Materials of Ministry of Education, Frontiers Science Center for Materiobiology and Dynamic Chemistry, School of Materials Science and Engineering, East China University of Science and Technology, Shanghai 200237, China;* orcid.org/0000-0001-9633-4483; Phone: +86-21-64253370; Email: jlin@ecust.edu.cn

Liquan Wang − *Shanghai Key Laboratory of Advanced Polymeric Materials, Key Laboratory for Ultrafine Materials of Ministry of Education, Frontiers Science Center for Materiobiology and Dynamic Chemistry, School of Materials Science and Engineering, East China University of Science and Technology, Shanghai 200237, China;* orcid.org/0000-0002-5141-8584; Email: lq_wang@ecust.edu.cn

Authors

Wei Hong − *Shanghai Key Laboratory of Advanced Polymeric Materials, Key Laboratory for Ultrafine Materials of Ministry of Education, Frontiers Science Center for Materiobiology and Dynamic Chemistry, School of Materials Science and Engineering, East China University of Science and Technology, Shanghai 200237, China*

Xiaohui Tian − *Shanghai Key Laboratory of Advanced Polymeric Materials, Key Laboratory for Ultrafine Materials of Ministry of Education, Frontiers Science Center for Materiobiology and Dynamic Chemistry, School of Materials Science and Engineering, East China University of Science and Technology, Shanghai 200237, China*

Complete contact information is available at: https://pubs.acs.org/10.1021/acs.jpcb.0c04235

Notes

The authors declare no competing financial interest.

■ ACKNOWLEDGMENTS

This work was supported by the National Natural Science Foundation of China (51833003, 51621002, 21774032, and 21975073).

■ REFERENCES

(1) Bouhfid, R.; Arrakhiz, F. Z.; Qaiss, A. Effect of Graphene Nanosheets on the Mechanical, Electrical, and Rheological Properties of Polyamide 6/Acrylonitrile−Butadiene−Styrene Blends. *Polym. Compos.* **2016**, *37*, 998−1006.

(2) Kashiwagi, T.; Mu, M.; Winey, K.; Cipriano, B.; Raghavan, S. R.; Pack, S.; Rafailovich, M.; Yang, Y.; Grulke, E.; Shields, J.; Harris, R.; Douglas, J. Relation between the Viscoelastic and Flammability Properties of Polymer Nanocomposites. *Polymer* **2008**, *49*, 4358−4368.

(3) Kim, J. K.; Yoon, K. H.; Bang, D. S.; Park, Y.-B.; Kim, H.-U.; Bang, Y.-H. Morphology and Rheological Behaviors of Poly(Ethylene Terephthalate) Nanocomposites Containing Polyhedral Oligomeric Silsesquioxanes. *J. Appl. Polym. Sci.* **2008**, *107*, 272−279.

(4) Song, P. a.; Yu, Y.; Zhang, T.; Fu, S.; Fang, Z.; Wu, Q. Permeability, Viscoelasticity, and Flammability Performances and Their Relationship to Polymer Nanocomposites. *Ind. Eng. Chem. Res.* **2012**, *51*, 7255−7263.

(5) Chen, Z.-K.; Yang, J.-P.; Ni, Q.-Q.; Fu, S.-Y.; Huang, Y.-G. Reinforcement of Epoxy Resins with Multi-Walled Carbon Nanotubes for Enhancing Cryogenic Mechanical Properties. *Polymer* **2009**, *50*, 4753−4759.

(6) Achaby, M. E.; Qaiss, A. Processing and Properties of Polyethylene Reinforced by Graphene Nanosheets and Carbon Nanotubes. *Mater. Des.* **2013**, *44*, 81−89.

(7) Song, Y.; Zheng, Q. Linear Rheology of Naonofilled Polymers. *J. Rheol.* **2015**, *59*, 155−191.

(8) Li, Y.; Kröger, M.; Liu, W. K. Nanoparticle Geometrical Effect on Structure, Dynamics and Anisotropic Viscosity of Polyethylene Nanocomposites. *Macromolecules* **2012**, *45*, 2099−2112.

(9) Sabzi, M.; Jiang, L.; Nikfarjam, N. Graphene Nanoplatelets as Rheology Modifiers for Polylactic Acid: Graphene Aspect-Ratio-Dependent Nonlinear Rheological Behavior. *Ind. Eng. Chem. Res.* **2015**, *54*, 8175−8182.

(10) Liao, K.-H.; Aoyama, S.; Abdala, A. A.; Macosko, C. Does Graphene Change T_g of Nanocomposites? *Macromolecules* **2014**, *47*, 8311−8319.

(11) Das, S.; Irin, F.; Ma, L.; Bhattacharia, S. K.; Hedden, R. C.; Green, M. J. Rheology and Morphology of Pristine Graphene/Polyacrylamide Gels. *ACS Appl. Mater. Interfaces* **2013**, *5*, 8633−8640.
(12) Dykes, L. M. C.; Torkelson, J. M.; Burghardt, W. R. Shear-Induced Orientation in Well-Exfoliated Polystyrene/Clay Nanocomposites. *Macromolecules* **2012**, *45*, 1622−1630.
(13) Kim, H.; Macosko, C. W. Morphology and Properties of Polyester/Exfoliated Graphite Nanocomposites. *Macromolecules* **2008**, *41*, 3317−3327.
(14) He, C.; She, X.; Peng, Z.; Zhong, J.; Liao, S.; Gong, W.; Liao, J.; Kong, L. Graphene Networks and Their Influence on Free-Volume Properties of Graphene-Epoxidized Natural Rubber Composites with a Segregated Structure: Rheological and Positron Annihilation Studies. *Phys. Chem. Chem. Phys.* **2015**, *17*, 12175−12184.
(15) Potts, J. R.; Murali, S.; Zhu, Y.; Zhao, X.; Ruoff, R. S. Microwave-Exfoliated Graphite Oxide/Polycarbonate Composites. *Macromolecules* **2011**, *44*, 6488−6495.
(16) Yu, T.; Lin, J.; Xu, J.; Chen, T.; Lin, S. Novel Polyacrylonitrile Nanocomposites Containing Na-Montmorillonite and Nano SiO_2 Particle. *Polymer* **2005**, *46*, 5695−5697.
(17) Patra, S.; Veettil, V. T.; Narayanan, T. N. Enhanced Viscoelastic Properties of Graphene Oxide Membranes. *Carbon* **2017**, *124*, 576−583.
(18) Niu, R.; Gong, J.; Xu, D.; Tang, T.; Sun, Z.-Y. Influence of Molecular Weight of Polymer Matrix on the Structure and Rheological Properties of Graphene Oxide/Polydimethylsiloxane Composites. *Polymer* **2014**, *55*, 5445−5453.
(19) Guimont, A.; Beyou, E.; Martin, G.; Sonntag, P.; Cassagnau, P. Viscoelasticity of Graphite Oxide-Based Suspensions in PDMS. *Macromolecules* **2011**, *44*, 3893−3900.
(20) Bian, J.; Lin, H. L.; He, F. X.; Wang, L.; Wei, X. W.; Chang, I.-T.; Sancaktar, E. Processing and Assessment of High-Performance Poly(Butylene Terephthalate) Nanocomposites Reinforced with Microwave Exfoliated Graphite Oxide Nanosheets. *Eur. Polym. J.* **2013**, *49*, 1406−1423.
(21) Wu, D.; Zhou, C.; Hong, Z.; Mao, D.; Bian, Z. Study on Rheological Behaviour of Poly(Butylene Terephthalate)/Montmorillonite Nanocomposites. *Eur. Polym. J.* **2005**, *41*, 2199−2207.
(22) Zhao, J.; Morgan, A. B.; Harris, J. D. Rheological Characterization of Polystyrene−Clay Nanocomposites to Compare the Degree of Exfoliation and Dispersion. *Polymer* **2005**, *46*, 8641−8660.
(23) Hyun, Y. H.; Lim, S. T.; Choi, H. J.; Jhon, M. S. Rheology of Poly(Ethylene Oxide)/Organoclay Nanocomposites. *Macromolecules* **2001**, *34*, 8084−8093.
(24) Tang, L.-C.; Wan, Y.-J.; Yan, D.; Pei, Y.-B.; Zhao, L.; Li, Y.-B.; Wu, L.-B.; Jiang, J.-X.; Lai, G.-Q. The Effect of Graphene Dispersion on the Mechanical Properties of Graphene/Epoxy Composites. *Carbon* **2013**, *60*, 16−27.
(25) Zhang, H.-B.; Zheng, W.-G.; Yan, Q.; Jiang, Z.-G.; Yu, Z.-Z. The Effect of Surface Chemistry of Graphene on Rheological and Electrical Properties of Polymethylmethacrylate Composites. *Carbon* **2012**, *50*, 5117−5125.
(26) Sadeghipour, H.; Ebadi-Dehaghani, H.; Ashouri, D.; Mousavian, S.; Hashemi-Fesharaki, M.; Shahbazi Gahrouei, M. Effects of Modified and Non-Modified Clay on the Rheological Behavior of High Density Polyethylene. *Composites, Part B* **2013**, *52*, 164−171.
(27) Hattemer, G. D.; Arya, G. Viscoelastic Properties of Polymer-Grafted Nanoparticle Composites from Molecular Dynamics Simulations. *Macromolecules* **2015**, *48*, 1240−1255.
(28) Shen, J.; Liu, J.; Li, H.; Gao, Y.; Li, X.; Wu, Y.; Zhang, L. Molecular Dynamics Simulations of the Structural, Mechanical and Visco-Elastic Properties of Polymer Nanocomposites Filled with Grafted Nanoparticles. *Phys. Chem. Chem. Phys.* **2015**, *17*, 7196−7207.
(29) Smith, G. D.; Bedrov, D.; Li, L.; Byutner, O. A Molecular Dynamics Simulation Study of the Viscoelastic Properties of Polymer Nanocomposites. *J. Chem. Phys.* **2002**, *117*, 9478−9489.
(30) Xu, Y.; Green, M. J. Brownian Dynamics Simulations of Nanosheet Solutions under Shear. *J. Chem. Phys.* **2014**, *141*, 024905.
(31) Zhang, Q.; Lin, J.; Wang, L.; Xu, Z. Theoretical Modeling and Simulations of Self-Assembly of Copolymers in Solution. *Prog. Polym. Sci.* **2017**, *75*, 1−30.
(32) Zhang, X.; Wu, L.; Wang, J. Distinct Mechanical Properties of Polymer/Polymer-Grafting-Graphene Nanocomposites. *Macromol. Chem. Phys.* **2018**, *219*, 1800161.
(33) Pryamitsyn, V.; Ganesan, V. Origins of Linear Viscoelastic Behavior of Polymer−Nanoparticle Composites. *Macromolecules* **2006**, *39*, 844−856.
(34) Xu, Z.; Lin, J.; Zhang, Q.; Wang, L.; Tian, X. Theoretical Simulations of Nanostructures Self-Assembled from Copolymer Systems. *Polym. Chem.* **2016**, *7*, 3783−3811.
(35) Li, Z.; Liu, J.; Zhang, Z.; Gao, Y.; Liu, L.; Zhang, L.; Yuan, B. Molecular Dynamics Simulation of the Viscoelasticity of Polymer Nanocomposites under Oscillatory Shear: Effect of Interfacial Chemical Coupling. *RSC Adv.* **2018**, *8*, 8141−8151.
(36) Xu, P.; Lin, J.; Zhang, L. Distinct Viscoelasticity of Nanoparticle-Tethering Polymers Revealed by Nonequilibrium Molecular Dynamics Simulations. *J. Phys. Chem. C* **2017**, *121*, 28194−28203.
(37) Jiang, T.; Wang, L.; Lin, J. Distinct Mechanical Properties of Nanoparticle-Tethering Polymers. *RSC Adv.* **2014**, *4*, 35272−35283.
(38) Rissanou, A. N.; Harmandaris, V. Dynamics of Various Polymer-Graphene Interfacial Systems through Atomistic Molecular Dynamics Simulations. *Soft Matter* **2014**, *10*, 2876−2888.
(39) Rissanou, A.; Power, A.; Harmandaris, V. Structural and Dynamical Properties of Polyethylene/Graphene Nanocomposites through Molecular Dynamics Simulations. *Polymers* **2015**, *7*, 390−417.
(40) Bačová, P.; Rissanou, A. N.; Harmandaris, V. Edge-Functionalized Graphene as a Nanofiller: Molecular Dynamics Simulation Study. *Macromolecules* **2015**, *48*, 9024−9038.
(41) Güryel, S.; Walker, M.; Geerlings, P.; De Proft, F.; Wilson, M. R. Molecular Dynamics Simulations of the Structure and the Morphology of Graphene/Polymer Nanocomposites. *Phys. Chem. Chem. Phys.* **2017**, *19*, 12959−12969.
(42) Wang, Q.; Keffer, D. J.; Nicholson, D. M.; Thomas, J. B. Coarse-Grained Molecular Dynamics Simulation of Polyethylene Terephthalate (PET). *Macromolecules* **2010**, *43*, 10722−10734.
(43) Dupuy, L. M.; Tadmor, E. B.; Miller, R. E.; Phillips, R. Finite-Temperature Quasicontinuum: Molecular Dynamics without All the Atoms. *Phys. Rev. Lett.* **2005**, *95*, 060202.
(44) Piserchia, A.; Zerbetto, M.; Salvia, M.-V.; Salassa, G.; Gabrielli, L.; Mancin, F.; Rastrelli, F.; Frezzato, D. Conformational Mobility in Monolayer-Protected Nanoparticles: From Torsional Free Energy Profiles to NMR Relaxation. *J. Phys. Chem. C* **2015**, *119*, 20100−20110.
(45) Zhang, Z.; Glotzer, S. C. Self-Assembly of Patchy Particles. *Nano Lett.* **2004**, *4*, 1407−1413.
(46) Liu, J.; Wu, S.; Zhang, L.; Wang, W.; Cao, D. Molecular Dynamics Simulation for Insight into Microscopic Mechanism of Polymer Reinforcement. *Phys. Chem. Chem. Phys.* **2011**, *13*, 518−529.
(47) Liu, J.; Cao, D.; Zhang, L. Molecular Dynamics Study on Nanoparticle Diffusion in Polymer Melts: A Test of the Stokes−Einstein Law. *J. Phys. Chem. C* **2008**, *112*, 6653−6661.
(48) Allen, M. P.; Tildesley, D. J. *Computer Simulation of Liquids*; Oxford University: New York, 1987.
(49) Chen, Y.; Li, Z.; Wen, S.; Yang, Q.; Zhang, L.; Zhong, C.; Liu, L. Molecular Simulation Study of Role of Polymer−Particle Interactions in the Strain-Dependent Viscoelasticity of Elastomers (Payne Effect). *J. Chem. Phys.* **2014**, *141*, 104901.
(50) Xu, P.; Lin, J.; Wang, L.; Zhang, L. Shear Flow Behaviors of Rod-Coil Diblock Copolymers in Solution: A Nonequilibrium Dissipative Particle Dynamics Simulation. *J. Chem. Phys.* **2017**, *146*, 184903.
(51) Doi, M.; Edwards, S. F. *The Theory of Polymer Dynamics*; Oxford University Press: New York, 1986.
(52) Gao, C.; Zhang, S.; Wang, F.; Wen, B.; Han, C.; Ding, Y.; Yang, M. Graphene Networks with Low Percolation Threshold in ABS

https://dx.doi.org/10.1021/acs.jpcb.0c04235
J. Phys. Chem. B 2020, 124, 6437−6447

Nanocomposites: Selective Localization and Electrical and Rheological Properties. *ACS Appl. Mater. Interfaces* **2014**, *6*, 12252−12260.
(53) Zhan, Y.; Long, Z.; Wan, X.; He, Y.; Liu, X. Exfoliated Graphite Nanoplatelets/Poly(Arylene Ether Nitrile) Nanocomposites: *In situ* Synthesis, Characterization, and Enhanced Properties. *High Perform. Polym.* **2017**, *29*, 1121−1129.

https://dx.doi.org/10.1021/acs.jpcb.0c04235
J. Phys. Chem. B 2020, 124, 6437−6447